



## Proton–hole excitation in the closed shell nucleus $^{205}\text{Au}$

Zs. Podolyák<sup>a,\*</sup>, G.F. Farrelly<sup>a</sup>, P.H. Regan<sup>a</sup>, A.B. Garnsworthy<sup>a</sup>, S.J. Steer<sup>a</sup>, M. Górska<sup>b</sup>, J. Benlliure<sup>c</sup>, E. Casarejos<sup>c</sup>, S. Pietri<sup>a</sup>, J. Gerl<sup>b</sup>, H.J. Wollersheim<sup>b</sup>, R. Kumar<sup>d</sup>, F. Molina<sup>e</sup>, A. Algora<sup>e,f</sup>, N. Alkhomashi<sup>a</sup>, G. Benzoni<sup>g</sup>, A. Blazhev<sup>h</sup>, P. Boutachkov<sup>b</sup>, A.M. Bruce<sup>i</sup>, L. Caceres<sup>b,j</sup>, I.J. Cullen<sup>a</sup>, A.M. Denis Bacelar<sup>i</sup>, P. Doornenbal<sup>b</sup>, M.E. Estevez<sup>c</sup>, Y. Fujita<sup>k</sup>, W. Gelletly<sup>a</sup>, H. Geissel<sup>b</sup>, H. Grawe<sup>b</sup>, J. Grębosz<sup>b,l</sup>, R. Hoischen<sup>m,b</sup>, I. Kojouharov<sup>b</sup>, S. Lalkovski<sup>i</sup>, Z. Liu<sup>a</sup>, K.H. Maier<sup>n,l</sup>, C. Mihai<sup>o</sup>, D. Mücher<sup>h</sup>, B. Rubio<sup>e</sup>, H. Schaffner<sup>b</sup>, A. Tamii<sup>k</sup>, S. Tashenov<sup>b</sup>, J.J. Valiente-Dobón<sup>p</sup>, P.M. Walker<sup>a</sup>, P.J. Woods<sup>q</sup>

<sup>a</sup> Department of Physics, University of Surrey, Guildford GU2 7XH, UK

<sup>b</sup> GSI, Planckstrasse 1, D-64291 Darmstadt, Germany

<sup>c</sup> Universidad de Santiago de Compostela, E-15706, Santiago de Compostela, Spain

<sup>d</sup> Inter University Accelerator Centre, New Delhi, India

<sup>e</sup> Instituto de Física Corpuscular, Universidad de Valencia, E-46071, Spain

<sup>f</sup> Institute for Nuclear Research, H-4001 Debrecen, Hungary

<sup>g</sup> INFN, Università degli Studi di Milano, I-20133 Milano, Italy

<sup>h</sup> IKP, Universität zu Köln, D-50937 Köln, Germany

<sup>i</sup> School of Environment and Technology, University of Brighton, Brighton BN2 4GJ, UK

<sup>j</sup> Departamento de Física Teórica, Universidad Autónoma de Madrid, E-28049 Madrid, Spain

<sup>k</sup> Department of Physics, Osaka University, Toyonaka, Osaka 560-0043, Japan

<sup>l</sup> The Henryk Niewodniczański Institute of Nuclear Physics, PL-31-342 Kraków, Poland

<sup>m</sup> Department of Physics, Lund University, S-22100 Lund, Sweden

<sup>n</sup> Department of Physics, University of West of Scotland, Paisley PA1 2BE, UK

<sup>o</sup> "Horea Hulubet" National Institute for Physics and Nuclear Engineering, RO-077125 Bucharest, Romania

<sup>p</sup> INFN-Laboratori Nazionali di Legnaro, Italy

<sup>q</sup> Department of Physics and Astronomy, University of Edinburgh, UK

### ARTICLE INFO

#### Article history:

Received 7 July 2008

Received in revised form 26 November 2008

Accepted 7 January 2009

Available online 10 January 2009

Editor: V. Metag

#### PACS:

25.70.Mn

27.80.+w

### ABSTRACT

The neutron-rich  $N = 126$  nucleus  $^{205}\text{Au}$  has been populated following the relativistic energy projectile fragmentation of  $E/A = 1$  GeV  $^{208}\text{Pb}$ , and studied via charged-particle decay spectroscopy. An internal decay with a transition energy of 907(5) keV and a half-life of  $T_{1/2} = 6(2)$  s has been identified through the observation of the corresponding  $K$  and  $L$  internal conversion electron lines. The 907 keV energy level corresponds to the  $\pi h_{11/2}^{-1}$  proton–hole state and decays both internally into the  $\pi d_{3/2}^{-1}$  ground-state and via  $\beta$  decay into  $^{205}\text{Hg}$ . The obtained data provides information on the evolution of single-proton hole energies which are vital inputs of shell model descriptions for nuclei around the  $^{208}_{82}\text{Pb}_{126}$  doubly magic core.

© 2009 Elsevier B.V. All rights reserved.

Studies of magic nuclei are of fundamental importance in our understanding of nuclear structure since they allow direct tests of the purity of shell model wave functions. Information on the single-particle energies can be derived from the experimental observables such as energies of the excited states and transition probabilities.

The doubly magic  $^{208}\text{Pb}$  nucleus, with 82 protons and 126 neutrons, provides the heaviest classic shell model core. Current experimental information on the neutron-rich  $N = 126$  nuclei is very scarce. The data on the excited states of proton–hole  $N = 126$  iso-

tones is restricted to three nuclei, namely:  $^{207}_{81}\text{Tl}$  [1],  $^{206}_{80}\text{Hg}$  [2] and  $^{204}_{78}\text{Pt}$  [3]. In the case of  $^{205}_{79}\text{Au}$ , only a tentative spin-parity of the groundstate is known [4,5]. The experimental information on the structure of these nuclei can be used as building blocks for calculating more complex configurations. More information is available, more robust predictions can be made on the properties of more neutron-rich species. These are of particular importance as the r-process path nuclei, experimentally unreachable in this mass region so far, are approached [6].

The lack of information on proton–hole nuclei compared to the  $^{208}\text{Pb}$  core arises from difficulties in populating such neutron-rich nuclei. Projectile fragmentation has proved to be an efficient tool to produce exotic nuclear species. When projectile fragmentation is combined with high sensitivity gamma detection arrays, struc-

\* Corresponding author.

E-mail address: z.podolyak@surrey.ac.uk (Zs. Podolyák).

ture information can be gained for otherwise inaccessible nuclei (e.g.  $^{204}\text{Pt}$  [3]). The highest sensitivity is achieved with decay spectroscopy. In this technique the delayed gamma rays are correlated with the individually identified ion, therefore minimising the associated background radiation [7–9]. Here we employed a different version of the technique. Conversion electron spectroscopy following relativistic energy fragmentation was performed (according to our knowledge) for the first time.

In this Letter results on the  $N = 126$  nucleus  $^{205}\text{Au}$  are reported. A beryllium target of thickness  $2.5 \text{ g/cm}^2$  was bombarded with an  $E/A = 1 \text{ GeV}$   $^{208}\text{Pb}$  beam provided by the SIS accelerator at GSI, Darmstadt, Germany. The nuclei of interest, populated in relativistic energy projectile fragmentation, were separated and identified using the FRagment Separator (FRS) [10] operated in *monochromatic* mode with a wedge-shaped aluminium degrader in the intermediate focal plane of the separator. Niobium foils were placed after both the target and the degrader in order to maximise the electron stripping.

The mass-to-charge ratio of the ions,  $A/q$ , was determined from their time of flight and magnetic rigidity measurements in the second part of the FRS. The measured change of the magnetic rigidity of ions before and after they passed through this degrader was used to obtain unambiguous charge identification. The energy deposition of the identified fragments, which gives information on  $Z$ , was measured as they passed through two gas ionisation chambers. By determining  $A/q$ , the charge state and  $Z$ , an unambiguous event-by-event identification has been obtained. The transmitted (and identified) ions were slowed down in a variable thickness aluminium degrader and finally stopped in an active catcher.

The catcher consisted of three 1 mm thick  $5 \times 5 \text{ cm}^2$  double sided silicon strip detectors. Each Si had 16 X-strips and 16 Y-strips. The catcher allowed for the detection of both the implanted ion and the subsequent charged particle decay. A charged-particle decay observed in a given pixel was correlated with the previous implant detected in the very same pixel. Due to the large number of pixels, correlation between the implanted ion and the subsequent charged particle decay could be obtained over periods longer than seconds. Semilogarithmic preamplifiers were used, providing linear amplification up to 10 MeV and logarithmic for the 10 MeV–3 GeV range. The linear part allowed for the spectroscopy of the charged particle decay and was calibrated using an open internal conversion electron  $^{207}\text{Bi}$  source, yielding an energy resolution of  $\text{FWHM} = 20 \text{ keV}$  and a minimum detection threshold of 150 keV [11]. The logarithmic part allowed for the determination of the implantation position and was calibrated with a pulser. For details on the Si catcher and its electronics see Ref. [11]. Scintillation detectors were placed both in front of and behind the catcher, allowing the offline suppression of the majority of fragments destroyed in the slowing down process.

The catcher was surrounded by the high-efficiency, high granularity RISING  $\gamma$ -ray spectrometer in the “Stopped Beam” configuration [12]. The array consists of 15 former Euroball cluster Ge detectors and has a full peak efficiency of 15% at 662 keV [12]. Time-correlated  $\gamma$  decays following both internal-decay and  $\beta$ -decay have been recorded. The experiment was monitored using the Cracow analysis software [13].

A dedicated fragment separator setting was used to study the neutron-rich  $^{205}\text{Au}$  nucleus. After the production target the magnetic rigidity of the fully stripped  $^{205}\text{Au}$  nuclei is close to those of the intense He-like primary  $^{208}\text{Pb}$  beam. In order to avoid this contamination, the first half of the fragment separator was set to transmit the H-like  $^{205}\text{Au}$  ions. Although only an estimated 6.5% of the ions of interest were in their H-like charged state [14], the high production cross section in the order of  $10^{-2} \text{ mbarn}$  [15] ensures sufficient statistics for the current measurement. In the second part of the fragment separator, after the monochromatic

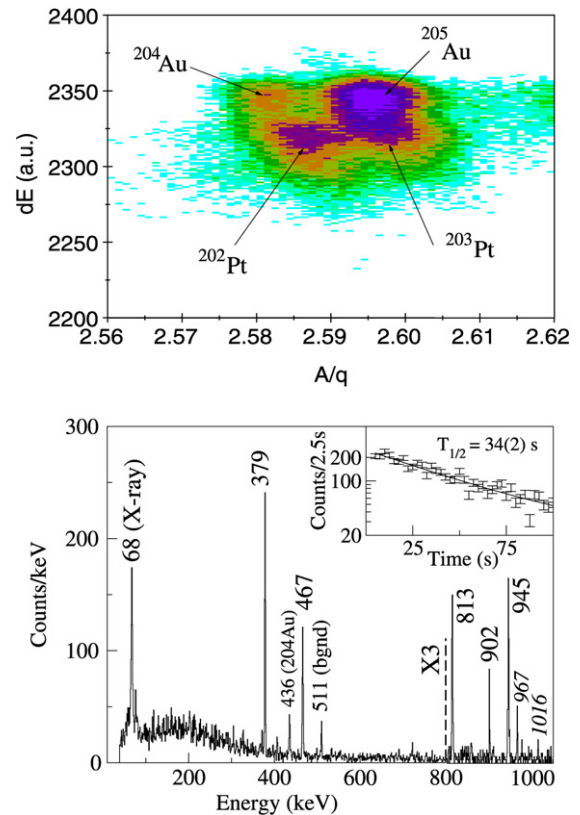


**Fig. 1.** (Top) Identification plot of the fragments of interest. (Bottom)  $\gamma$ -ray spectrum associated to the  $\beta$  decay of the  $^{205}\text{Au}$  ions using a maximum implantation-decay correlation time of 5 s. The labelled peaks, unless stated otherwise, belong to  $^{205}\text{Hg}$  [5] and confirm the identification. The peaks labelled in normal letters originate from the previously studied  $\beta$  decay of the  $^{205}\text{Au}$  groundstate [4], with the inset showing the corresponding decay curve. The peaks labelled in *italic* are associated with the  $\beta$  decay of the isomeric state of  $^{205}\text{Au}$  observed in the present work. For details see the text.

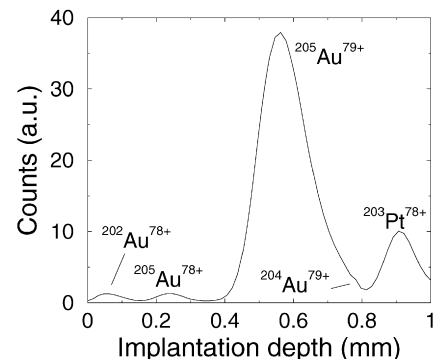


**Fig. 2.** Simulated implantation profile in the 1 mm thick Si detector.

degrader,  $^{205}\text{Au}$  was transmitted in its fully stripped charged state. This setting provided a beam consisting predominantly ( $\sim 55\%$ ) of  $^{205}\text{Au}$  nuclei, as shown in Fig. 1.

The primary  $^{208}\text{Pb}$  beam intensity was  $7 \times 10^8$  ion/spill, with the spill consisting of 1 s beam-on period followed by 10 s beam-off. The average implantation yield was  $\sim 30$   $^{205}\text{Au}$  ion/spill, corresponding to a total of  $76 \times 10^3$  collected ions. The observation of the previously identified  $\gamma$ -ray transitions in  $^{205}\text{Hg}$  in coincidence with the  $\beta$ -decay of the ground-state  $^{205}\text{Au}$  [4] confirmed the identification (see Fig. 1).

The use of the fragment separator in monochromatic mode allowed for the implantation of  $^{205}\text{Au}$  in a thin layer of Si, maximising the efficiency of the charged particle detection. Fig. 2 shows the

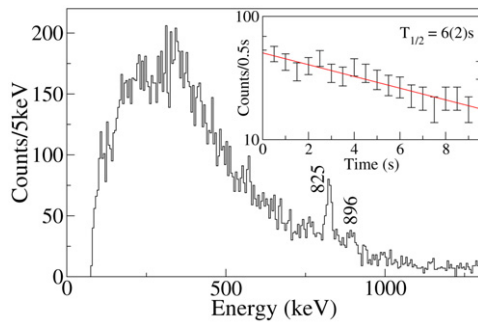


**Fig. 3.** Delayed charged particle spectrum associated to  $^{205}\text{Au}$ . In addition to the continuous energy of the  $\beta$  decay, two peaks are observed. These are interpreted as  $K$  and  $L$  internal conversion electron peaks corresponding to a 907(5) keV transition.

simulated range distribution within the 1 mm thick silicon detector. According to these simulations, performed with the LISE code [16], 70% of the implanted ions were  $^{205}\text{Au}$ . The delayed charged particle spectrum measured in the Si detector and correlated to the implanted  $^{205}\text{Au}$  ions is presented in Fig. 3. In addition to the continuous energy spectrum of the  $\beta$  electron from the  $^{205}\text{Au}$  decay, two discrete peaks can be observed. These are interpreted as the  $K$  and  $L$  internal conversion electrons associated to a  $\gamma$ -ray transition with an energy of 907(5) keV. (Note that the  $L$  line contains contribution from the weak and unresolved  $M, N, \dots$  lines.) The energy difference between the  $K$  and  $L$  lines, as well as the intensity ratio of the two peaks supports this interpretation. The measured lifetime of the decay is  $T_{1/2} = 6(2)$  s. This lifetime suggests a transition with  $M4$  or  $E4$  character (considering a transition strength between  $10^{-4}$  and  $10^{+3}$  W.u.).

The  $\gamma$ -ray spectrum associated to the  $\beta$  decay of  $^{205}\text{Au}$  is shown in Fig. 1. When compared with that of the previous study of Ch. Wennemann et al. [4], one notices that the spectrum contains two additional transitions with energies of 967 and 1016 keV. These  $\gamma$  lines are clearly visible when a maximum implantation-decay correlation time in the order of seconds is used (5 s in Fig. 1), and they disappear in the background if a much longer maximum correlation time is chosen. These  $\gamma$  lines were previously identified in  $^{205}\text{Hg}$  (but not from  $\beta$  decay) and they deexcite states with spin-parities  $7/2^-$  and  $9/2^-$ , respectively [5]. These spins are high when compared to that of the  $3/2^+$  groundstate of  $^{205}\text{Au}$ , therefore it is unlikely that these  $\gamma$ -ray transitions originate from the  $\beta$  decay of the  $^{205}\text{Au}$  groundstate. The lifetimes associated to these two  $\gamma$ -ray transitions are consistent with the 6 s half-life of the conversion electron, and in the case of the stronger 967 keV transition inconsistent with the much longer lifetime of the groundstate  $\beta$  decay. All these experimental findings suggest the identification of an isomeric state in  $^{205}\text{Au}$ , and that this state decays both internally and via  $\beta$  decay. The branching ratio between these decays cannot be determined due to poor knowledge of the full peak conversion electron detection efficiency.

The proton-hole orbitals below the  $Z = 82$  closed proton shell are  $s_{1/2}$ ,  $d_{3/2}$ ,  $h_{11/2}$ ,  $d_{5/2}$  and  $g_{7/2}$ . The experimental level scheme of the  $Z = 81$ ,  $N = 126$  single-hole  $^{207}\text{Tl}$  nucleus gives a clear graphical demonstration of this, as shown in Fig. 4.  $^{205}\text{Au}$  is a three proton-hole nucleus, with an expected groundstate configuration of  $\pi d_{3/2}^{-1}$  (with the  $s_{1/2}$  being empty) and spin-parity  $I^\pi = 3/2^+$ . The  $\pi h_{11/2}$  excited state should be long lived since it can decay only through high multipolarity transitions, similarly like in  $^{207}\text{Tl}$ . Accordingly, the transition observed in the present experiment should originate from the decay of the  $11/2^-$  isomeric state. The experimentally identified 907(5) keV transition corresponds to the  $11/2^- \rightarrow 3/2^+$  transition of  $M4$  character and a theoretical internal conversion coefficient [21] of  $\alpha = 0.18$ . The relatively high

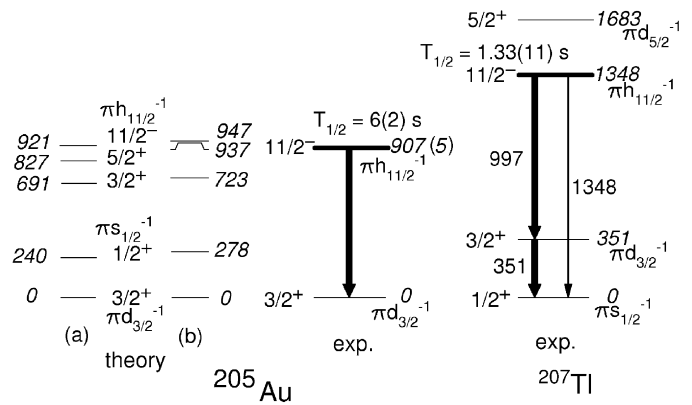


**Fig. 4.** Calculated and experimental level schemes of  $^{205}\text{Au}$ . Calculations have been performed using both the standard set of matrix elements of Ref. [18] (labelled (a)) and a modified set optimised for the description of  $^{204}\text{Pt}$  [3] (labelled (b)). For comparison the partial level scheme of  $^{207}\text{Tl}$  is also given [1].

electron conversion coefficient together with the high energy of the transition, a rare combination, made possible the identification of this transition with the present method.

In order to obtain a quantitative understanding of the underlying single-particle structure of the excited states of  $^{205}\text{Au}$ , shell-model calculations have been performed employing the OXBASH code [17]. The standard interaction two-body matrix elements (TBMEs) were used as taken from Ref. [18]. They are based on the Kuo–Brown interaction including core polarisation [19,20], with slight modifications introduced to obtain an improved description of the experimental data available at the time. The proton-hole energies were taken from the experimental level scheme of  $^{207}\text{Tl}$  [1]. This parameterisation gives a good description of the reported excited states in the two proton-hole  $^{206}\text{Hg}$  [2] and reasonable description for the four proton-hole nucleus  $^{204}\text{Pt}$  [3]. In order to get a good description for all available information on the  $N = 126$  isotones below lead, both on excitation energies and transition strengths, small modifications of the standard TBMEs were required [3]. Calculations with these modified matrix elements were also performed. The results of the calculations for  $^{205}\text{Au}$ , using both sets of TBMEs, are compared with the experimental level schemes in Fig. 4. The dominant configurations are also indicated.

The measured energy of the isomeric state with the proposed  $11/2^-$  spin-parity is in good agreement with the shell model calculations. The calculations also predict a  $5/2^+$  state to lie below the  $11/2^-$  isomer, therefore the isomer could decay into it via an  $E3$  transition. The Weisskopf estimate for the partial lifetime of this transition is in the order of 0.1 s. This transition, even if it exists, could not be observed in the present experiment: the energy of the corresponding conversion electron is low and could not be discerned from the background; the  $\gamma$  branch could have not been correlated with the  $^{205}\text{Au}$  ions due to the long lifetime of the isomer. As a consequence, the  $M4/E3$  branching ratio could not be ascertained in the current work. Since the  $11/2^-$  isomeric state  $\beta$  decays and possibly decays internally through an  $E3$  branch, only an upper limit for the  $B(M4)$  transition strength was determined,  $B(M4) \leq 1.7(7)$  W.u. This limit is somewhat lower than that of the equivalent  $M4$  transition strength,  $3.2(3)$  W.u. [1], in  $^{207}\text{Tl}$ , and similar to those determined in lighter gold isotopes:  $2.4(8)$  W.u. in  $^{197}\text{Au}$  [22] and  $2.2(3)$  W.u. in  $^{195}\text{Au}$  [23]. This suggests that the  $E3$  branching might be missing altogether, possible because the  $5/2^+$  state lies above the  $11/2^-$  isomer.

In conclusion, an excited state in the neutron-rich  $N = 126$   $^{205}\text{Au}$  nucleus has been identified through conversion electron spectroscopy. It has an excitation energy of 907(5) keV and a half-life of  $T_{1/2} = 6(2)$  s. It corresponds to the  $\pi h_{11/2}^{-1}$  single proton-

hole excitation and decays both internally into the  $\pi d_{3/2}^{-1}$  ground-state and via  $\beta$  decay into excited states of  $^{205}\text{Hg}$ . The energy of the isomeric state is in good agreement with the shell-model calculations.

### Acknowledgements

The excellent work of the GSI accelerator staff is acknowledged. This work is supported by the EPSRC (UK), STFC (UK), the EU Access to Large Scale Facilities Programme (EURONS, EU contract 506065), The Spanish Ministerio de Educacion y Ciencia and The German BMBF.

### References

- [1] D. Eccleshall, M.J.L. Yates, Phys. Lett. 19 (1965) 301; M.J. Martin, Nucl. Data Sheets 70 (1993) 315.
- [2] B. Fornal, et al., Phys. Rev. Lett. 87 (2001) 212501.
- [3] S. Steer, et al., Phys. Rev. C 78 (2008) 061302(R).
- [4] Ch. Wennemann, et al., Z. Phys. A 347 (1994) 185.
- [5] F.G. Kondev, Nucl. Data Sheets 101 (2004) 521.
- [6] H. Grawe, K. Langanke, G. Martinez-Pinedo, Rep. Prog. Phys. 70 (2007) 1525.
- [7] R. Grzywacz, et al., Phys. Lett. B 335 (1995) 439.
- [8] M. Pfützner, et al., Phys. Lett. B 444 (1998) 32.
- [9] Zs. Podolyák, et al., Phys. Lett. B 491 (2000) 225.
- [10] H. Geissel, et al., Nucl. Instrum. Methods Phys. Res. Sect. B 70 (1992) 286.
- [11] R. Kumar, et al., Nucl. Instrum. Methods A 598 (2009) 754.
- [12] S. Pietri, et al., Nucl. Instrum. Methods B 261 (2007) 1079; P.H. Regan, et al., Nucl. Phys. A 787 (2007) 491c.
- [13] J. Grebosz, Comput. Phys. 176 (2007) 251.
- [14] C. Scheidenberger, et al., Nucl. Instrum. Methods B 142 (1998) 441.
- [15] L. Audouin, et al., Nucl. Phys. A 768 (2006) 1.
- [16] D. Bazin, O. Tarasov, M. Lewitowicz, O. Sorlin, Nucl. Instrum. Methods A 482 (2002) 307.
- [17] B.A. Brown, A. Etchegoyen, W.D.M. Rae, The computer code OXBASH, MSU-NSCL report number 524.
- [18] L. Rydström, et al., Nucl. Phys. A 512 (1990) 217.
- [19] T.T.S. Kuo, G.H. Herling, Naval Research Laboratory Report 2259 (Washington, DC, 1971).
- [20] G.H. Herling, T.T.S. Kuo, Nucl. Phys. A 181 (1972) 113.
- [21] T. Kibédi, T.W. Burrows, M.B. Trzhaskovskaya, C.W. Nestor Jr., AIP Conf. Proc. 769 (2005) 268.
- [22] X. Huang, C. Zhou, Nucl. Data Sheets 104 (2005) 283.
- [23] C. Zhou, Nucl. Data Sheets 86 (1999) 645.